33rd Annual International Conference of the IEEE EMBS
Boston, Massachusetts USA, August 30 - September 3, 2011

Thermal Infrared Imaging: Toward Diagnostic Medical Capability

Daniel TJ. Arthur and Masood Mehmood Khan

***Abstract*— Thermal infrared imaging (TIRI) employs a focal plane array (FPA) of infrared detectors, with associated optics and optoelectronics to remotely detect and topographically map thermal emittance. Thermal and optical properties of human physioanatomy are not fully understood yet confounding diagnostic interpretation of human TIRI's. Elucidation of the specific physical mechanism via which thermal emission arises from human anatomy in-vivo requires empirical investigation under objective clinical protocols. This paper characterizes the fundamental architecture of the clinical TIRI system with a view to facilitation of objective protocol development, elucidation of the mechanism/s of human thermal infrared emittance, and eventual validation of TIRI as a diagnostic medical tool. Relevant recent and ongoing empirical studies by the authors are also summarized.**

I. Introduction

THERMAL infrared imaging (TIRI) employs a focal plane array of infrared detectors, with associated optics and readout circuitry to remotely detect and topographically map thermal emittance. A body's thermal emittance ($W/m^2/\mu m$) is a function of both temperature and emissivity, where emissivity (ϵ) is an index value from 0-1 describing ability of a surface to emit energy via radiation relative to a perfect blackbody radiator. The passive, non-invasive, non-ionizing nature of TIRI has raised interest in potential applications in medicine. The specific mechanism/s of spectral human emittance are currently poorly understood, precluding meaningful interpretation of clinical TIRI's. This paper characterizes the fundamental architecture of the clinical TIRI system (Fig. 1) with a view to facilitation of objective protocol development, elucidation of the mechanism of human thermal infrared emittance, and eventual validation of TIRI as a diagnostic medical tool. With objective validation, such a tool would find widespread application in non-invasive; diagnostics, prognostics, biometrics, patient monitoring, and surgery [1-3].

Manuscript received April 12, 2011.

Masood Mehmood Khan is with the Faculty of Science and Engineering, Curtin University of Technology, Perth, WA 6102, AUS, phone: +61 8 9266 9205; e-mail: masood.khan@curtin.edu.au

D. TJ. Arthur is with the Department of Mechanical Engineering, Curtin University of Technology Perth, WA 6102, AUS, phone: +61 8 9266 2886; e-mail: d.arthur@postgrad.curtin.edu.au

At the 2010 EMBC workshop entitled 'Lessons Learned from Medical Systems Development', several pertinent contemporary issues were raised, namely that; currently available methods for inference of spatiotemporal tissue-temperature profiles, as used in development of tumor ablation devices, are costly and difficult to implement; emphasis must be placed upon both lower-priced and faster alternatives to existing systems with similar function; and that a winning medical system design must gain acceptance from all stakeholders [4].

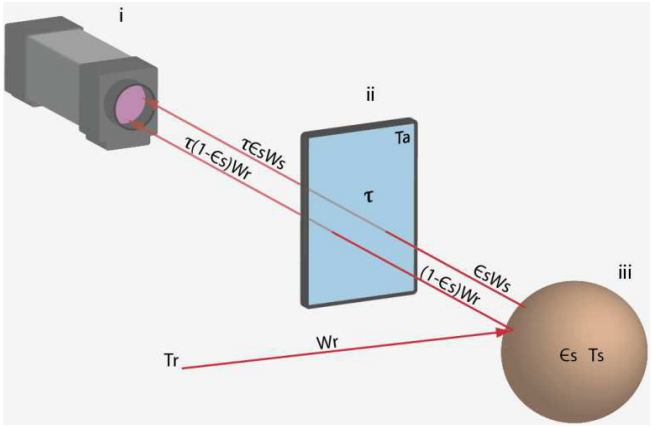

Fig. 1. Schematic representation of the clinical TIR image acquisition system architecture. The 3 subsystem entities shown include i) the thermal camera (FPA + associated optoelectronics), ii) the ambient atmosphere, and iii) the tissue volume of interest. Where; T_r = temperature of ambient sources, $\tau(1-\epsilon_s)W_r$ = TIR radiation from ambient sources reaching the lens of the camera, $\tau\epsilon_s W_s$ = TIR radiation from human subject reaching the lens, W_r = emittance from ambient sources, τ = atmospheric transmittance, T_a = temperature of ambient atmosphere, $(1-\epsilon_s)W_r$ = emittance from human tissue due to reflection of radiation from ambient sources, $\epsilon_s W_s$= emittance from human tissue due to intrinsic temperature and emissivity, ϵ_s= emissivity of tissue volume, T_s = surface temperature of tissue volume.

II. Tissue Volume of Interest

Diagnostic interpretation of human TIRI's will require accurate dynamic modelling of both the thermal and optical properties of the physioanatomic milieu. Existing models attempt to characterize transient 3D tissue temperature profiles in terms of conduction and convection, based upon allocation of the thermal topography of the TIRI to the outer surface of

the skin, and application of augmented versions of Pennes' Bioheat Equation (1) to computational bioheat transfer models as represented by Fig. 2.

$$\rho_n C_n \frac{\partial T_n}{\partial t} = k_n \nabla^2 T_n + \rho_b C_b \omega_b (T_b - T_n) + Q_n \quad (1)$$

Equation 1: Pennes' Bioheat equation describing transient temperature distribution within human tissue layers of thickness 'n', where ρ_n = tissue density, C_n = specific heat of tissue, T_n = local tissue temperature, k_n = tissue thermal conductivity, Q_n = metabolic heat generation per unit tissue volume, ρ_b = blood density, C_b = blood specific heat, ω_b = blood perfusion rate, and T_b = arterial blood temperature [5].

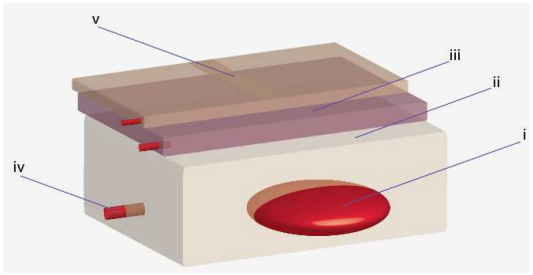

Fig. 2. Schematic cross-sectional depiction of a generic volume of interest (VOI), featuring; i) the lesion/kill-zone at the pathothermal hypocenter; ii) the lesion's host tissue/s; iii) interstitial tissue/s; iv) embedded vascular network; and v) the pathothermal epicenter on the outer surface of the superficial tissue layer, constituting the thermal infrared region of interest (ROI).

Current bioheat modelling research is focussed upon development of algorithmic arguments to accurately account for the dominant processes involved in the arterial transport phenomenon [6]. Most prominent among these are the Staverman filtration and osmotic reflection coefficients, accounting for selective rejection of species by the endothelium and internal elastic lamina, porous membranes, and the effects of osmotic pressure. Also of interest are the mechanical effects of blood flow upon heat transfer characteristics of the lumen and arterial wall, with the porous-media approach currently in favour [7].

Considering optical properties, in-vivo TIRI of the in-tact human body is highly illumination invariant, implying a large degree of bodily absorption and correspondingly high effective emissivity [8]. Recent studies have reported significantly greater thermal emission from a human body with an outer surface temperature of 32℃, than from a blackbody in the same scene, also with an outer surface temperature of 32℃ [8]. As a real graybody cannot emit more efficiently than a blackbody of equal surface temperature, the outer skin layer cannot be considered the sole graybody source for the imaged emittance from a human body. This phenomenon tends to agree with the independence of visible skin colour and bodily thermal emissivity [8].

The authors are currently investigating the specific phenomenology of human emittance, aswell as the correlation of TIRI 'hotspots' to MRI signs of osseous stress

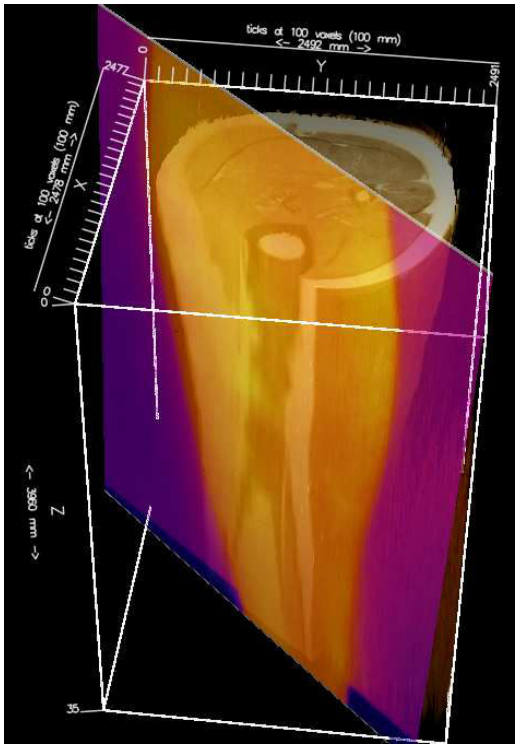

Fig. 3. Validation of TIRI aberration due to tibial stress injury [9] via intrasubject registration of 2D TIRI to cortico-periosteal interface in 3D MRI volume. 3D MRI model generation and TIRI registration are being performed within the AvisoFire and Drishti-2 volume exploration environments at the iVEC supercomputing facility.

pathophysiology via registration of thermographic, spectroscopic, and normal magnetic resonance sequences to multispectral 2D TIRI data, as illustrated in Fig 3. As the specific mechanism/s of human emittance are currently unknown, the biosignal of interest (Fig. 1, $\epsilon_s W_s$) may best be characterized in terms of the spectral power distributions and measurement wavebands shown in Fig. 4, showing the two relevant measurement wavebands, the interstitial band of atmospheric opacity and the spectral power distribution of skin within characteristic temperature range.

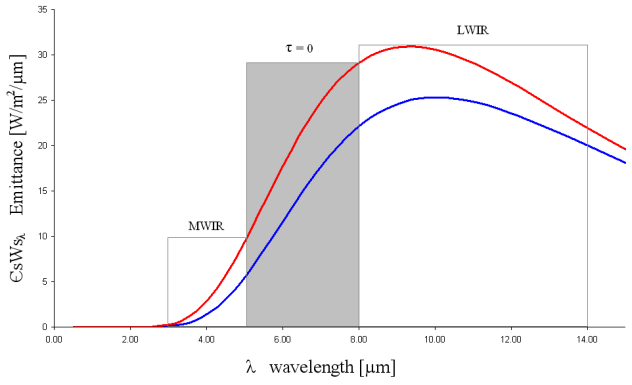

Fig. 4. Spectral power distributions of human tissues as characterized in context of TIRI within approximately characteristic pathophysiological temperature range (18-40°C). Relevant measurement bandwidths are shown; 3-5µm MWIR, 5-8µm band of atmospheric opacity, 8-14µm LWIR.

III. Ambient Clinical Atmosphere

The ambient clinical image-acquisition atmosphere (Fig. 1ii) serves as; an optical medium for interacting TIR signals, a source of TIR noise, a dictator of FPA performance, and a set of thermophysiological stimuli to the tissue volume.

A. As an Optical Medium

As aforementioned, the 5-8µm band between the (Figs. 4 and 5) is almost completely opaque to the IR signal of interest. Figure 4 shows 0% transmission within the 5.4-7.6µm band due to the absorption of IR by atmospheric H_2O molecules [10]. The MWIR and LWIR wavebands feature varying degrees of absorption due to atmospheric H_2O, CO_2, and O_2, but remain significantly transmissive (>80%) for the most part.

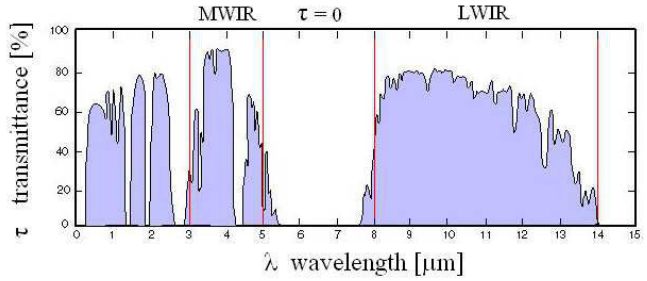

Fig. 5 Spectral atmospheric transmittance corresponding to 'τ' in Fig. 1ii above. Red vertical lines showing wavebands corresponding to Fig. 3; a) 3-5µm MWIR, (b) 5-8µm atmospheric opacity, (c) 8-14µm LWIR. Adapted from [10].

B. As a Source of IR Noise

A comprehensive analysis of the factors dictating the emissivity and temperature of the atmosphere is beyond the scope of this paper. It should however be noted that illumination invariance in the LWIR is not completely ideal, and identification of optimal illumination parameters requires further investigation [8].

C. As Thermophysiological Stimuli

Determination of optimal ambient conditions for pre image-acquisition equilibration or during image acquisition itself has received little attention [11-13]. As a general baseline it will likely be desirable, at least in context of equilibration, to foster thermoneutral conditions within which thermoregulation is actuated almost solely by peripheral vasomotion, with extremely limited perspiration, no shivering, and minimal catabolic thermogenesis. Recent efforts to establish these conditions have coupled CFD indoor-environment models (Fig.5a), with biocybernetic finite-element human thermoregulation models (Fig.5b) to simulate the overall thermal interaction between a human body and it's climate-controlled host indoor environment [14, 15]. Successive iterations of the IESD-Fiala model (Fig.5b) predict the thermal response of the body to the current ambient conditions provided by ANSYS CFX (Fig.5a). The resultant new skin surface properties are then fed back to CFX as inputs, with continued bidirectional iterations until a degree of convergence is reached, indicating thermoneutral conditions, as shown in Table 1.

TABLE I
Thermoneutral Environmental Conditions

T_{air}, °C	T_{sr}, °C	V_{air}, m/s	Rh, %	C_{wall},	act_{bas}, met
30.0	30.0	0.05	40.0	0.93	0.8

Atmospheric conditions required to facilitate human thermoneutrality T_{air}, ambient air temperature; T_{sr}, temperature of surrounding surfaces; V_{air}, ambient air velocity; rh, relative humidity; C_w, emissivity of surrounding wall surfaces; $act_{bas,}$ coefficient of metabolism due to physical exertion.

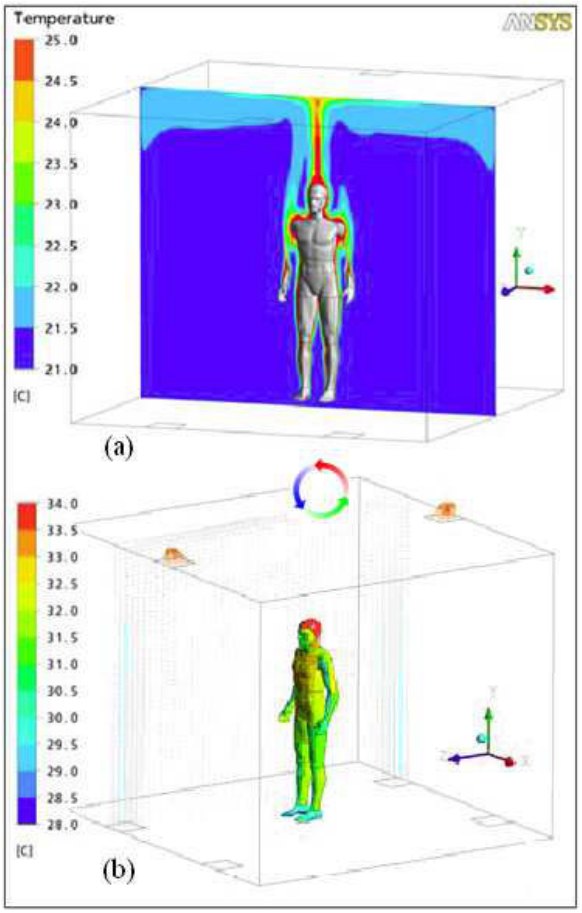

Fig. 6. (a) ANSYS CFX CFD model of flow and heat-transfer of air within a controlled indoor environment in which a ideal human body (grey manikin) is the sole heat source; showing the thermal plume within ambient air in the coronal plane correlating to the false-color temperature scale (℃); (b) IESD-Fiala cybernetic model predicting thermoregulatory reaction of the human central to a prescribed indoor environment as manifested at the skins surface; mean skin surface temperatures represented by false-color temperature scale (℃); thermal plumes of the environmental control system are shown in light blue at floor-level inlets and deep orange at ceiling outlets. Adapted with permission from [15].

IV. Thermal Infrared Camera

Until the precise mechanisms of human TIR emittance have been elucidated, evaluation of thermal camera suitability is limited to satisfaction of prerequisite spectral sensitivity requirements (MWIR or LWIR) and focal plane array (FPA) performance as characterised by the noise equivalent temperature difference index (NETD) (2).

$$NETD = (\tau C \eta_{BLIP} \sqrt{N_W})^{-1} \quad (2)$$

Equation 2: Noise equivalent temperature difference, where; τ = optical transmittance, C = thermal contrast, η_{BLIP} = ratio of photon noise to composite FPA noise, N_w = the number of photogenerated carriers integrated for one integration time [16].

$$N_W = \eta A_d t_{\text{int}} Q_b \quad (3)$$

Equation 3: Where N_w describes the number of photogenerated carriers integrated for one integration time in terms of the photon flux density (Q_b) incident upon the FPA's detector area (A_d) integrated during one integration time (t_{int}).

In the wavelength regions of interest, the three main third generation (current) detector technologies to consider are the cryo-cooled HgCdTe and antimonide based type-II superlattices, and the uncooled VO_x microbolometer arrays, with HgCdTe currently offering the highest performance at the greatest financial cost [16]. With a view to elucidation of TIR biosignal phenomenology, the cheaper uncooled technologies may be sufficient for qualitative proofs of concepts, although the superior performance currently offered by cooled technologies is preferable.

V. Conclusion

Thermal infrared imaging holds potential to be of great benefit within several areas of modern clinical medicine as a non-invasive physiological imaging modality. In order to realize this potential, the specific physical mechanisms of TIR emittance from human anatomy must be elucidated. Clinical TIRI must also undergo a rigorous holistic systems analysis, from which objective clinical protocols and contextual best practices may be established. This paper articulates the fundamental architecture of the clinical TIRI system, quantitatively characterizing the salient technological and biological factors. The many areas requiring further investigation are highlighted, with the state of the art alluded to. The authors are currently investigating the specific physical phenomenology of human MWIR and LWIR emittance, via registration of hyperspectral TIRI's to various thermographic magnetic resonance sequences (Fig. 3), This paper was written following the authors' recent clinical experience at the Australian Army Health centre, where they conducted a three month clinical investigation into application of TIRI to diagnosis and management of osseous stress pathology in the limbs of basic trainees under Australian Defence Force Human Research protocol 592-10, and Curtin University HREC Protocol HR62/2010.

Acknowledgment

The authors would like to thank Dr Andrew Squelch for his valuable time, insight, and facilitation of access to the iVEC supercomputing facility.

References

[1] C. Herman and M. Purtini Çetingül, "In-vivo detection of skin cancer using the dynamic infrared imaging technique," Journal of Heat Transfer-Transactions of ASME, vol. (accepted) 2011.

[2] L. de Weerd, "Free perforator flap surgery and dynamic infrared thermography - a clinical and experimental study," in Faculty of health sciences department of medical biology Tromso: University of Tromso, 2010.

[3] M. M. Khan, R. Ward, and M. Ingleby, "Classifying Pretended and Evoked Facial Expressions of Positive and Negative Affective States using Infrared Measurement of Skin Temperature," ACM Transactions on Applied Perception, vol. 6, pp. 1-22, 2009.

[4] X. Kong, N. Chbat, D. Haemmerich, M. Kroll, and D. Panescu, "Innovative Engineering Solutions: Lessons Learned from Medical Systems Development," in IEEE PULSE. vol. Jan/Feb, 2011, pp. 34-38.

[5] H. Pennes, "Analysis of tissue and arterial blood temperature in the resting human forearm," Applied Phsiology, vol. 85, pp. 93-122, 1948.

[6] O. Craciunescu and S. Clegg, "Pulsatile blood flow effects on temperature distribution and heat transfer in rigid vessels," Biomechanical Engineering, vol. 123, pp. 500-505, 2001.

[7] K. Khanafer and K. Vafai, "Synthesis of Mathematical Models Representing Bioheat Transport," in Advances in Numerical Heat Transfer. vol. 3, W. Minkowycz, E. Sparrow, and J. Abraham, Eds.: CRC Press, 2009.

[8] L. Wolff, D. Socolinsky, and C. Eveland, "Chapter 6: Face Recognition in the Thermal Infrared," in Computer Vision and Pattern Recognition Workshop on Computer Vision Beyond the Visible Spectrum Kauai, 2001.

[9] D. Arthur, M. M. Khan, and L. Barclay, "Thermographic Investigation of Osseous Stress Pathology," in IEEE Engineering in Medicine and Biology, Boston MA, 2011.

[10] P. Works, "Astrophysical Chemistry: Telluric Absorption ": Release #548, 2007.

[11] N. Zaproudina, V. Varmavuo, Airaksinen, and M. Närhi, "Reproducibility of infrared thermography measurements in healthy individuals. Physiological Measurement," Physiological Measurement vol. 29, pp. 515-524, 2008.

[12] R. Roy, J. Boucher, and A. Comtois, "Digitized Infrared Segmental Thermometry: Time Requirements for Stable Recordings Manipulative and Physiological Therapeutics," Manipulative and Physiological Therapeutics, vol. 29, pp. 468e1-469e10, 2006.

[13] M. Borten, B. Ransil, L. Di Leo, and E. Friedman, "Equilibration between breast surface and ambient temperature by liquid crystal thermography," Journal Of Reproductive Medicine, vol. 29(9):665-9, pp. 665-669, 1984.

[14] D. Nelson, S. Charbonnel, A. Curran, E. Marttila, and D. Fiala, "A High-Resolution Voxel Model for Predicting Local Tissue Temperatures in Humans Subjected to Warm and Hot Environments," Journal of Biomechanical Engineering, vol. 131, 2009.

[15] D. Fiala, A. Psikuta, G. Jendritzky, S. Paulke, D. Nelson, W. van Marken Lichtenbelt, and A. Frijns, "Physiological modeling for technical, clinical and research applications," Frontiers in Bioscience, vol. 2, pp. 939-968, 2010.

[16] A. Rogalski, "Recent progress in infrared detector technologies," Infrared Physics & Technology, 2011.